

84/2002

Raport Badawczy

RB/18/2002

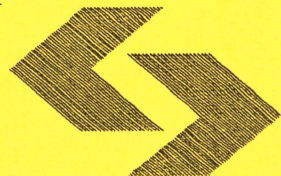
Research Report

**Evaluation of Environmental
Impact of Air
Pollution Sources**

P. Holnicki

**Instytut Badań Systemowych
Polska Akademia Nauk**

**Systems Research Institute
Polish Academy of Sciences**



POLSKA AKADEMIA NAUK

Instytut Badań Systemowych

ul. Newelska 6

01-447 Warszawa

tel.: (+48) (22) 8373578

fax: (+48) (22) 8372772

Kierownik Pracowni zgłaszający pracę:
Dr inż. Piotr Holnicki

Warszawa 2002

Evaluation of environmental impact of air pollution sources

Piotr Holnicki
Systems Research Institute
Polish Academy of Sciences, Warsaw

Keywords: air pollution, environment protection, mathematical modeling

Abstract: The paper addresses the problem of evaluation and comparison of environmental impact of emission sources in case of a complex, multi-sources emission field. The approach is based on the forecasts of a short-term, dynamic dispersion model. The aim is to get quantitative evaluation of the contribution of the selected sources, according to the specified environmental cost function. The approach utilizes the optimal control technique for distributed parameter systems. The adjoint equation, related to the main transport equation of the forecasting model, is applied to calculate the sensitivity of the cost function to the emission intensity of the specified sources. An example implementation of a regional scale, multi-layer dynamic model of SO_x transport is discussed as the main forecasting tool. The test computations have been performed for a set of the major power plants in a selected industrial region of Poland.

1 General formulation of the problem

The most common application of environmental models is forecasting of dispersion of pollutants. Air quality studies are also aimed at optimization, but numerous applications of optimization methods occur in the design of monitoring networks. On the other hand, many important decisions in air pollution and environmental problems are made by decision makers and not by the respective models. Some optimization methods and environmental models give the possibility of implementation of air pollution control strategies [4, 5]. For example, the optimal strategy for emission reduction or the real-time emission control can be worked out basing on the respective model solution. The algorithms that solve such problems usually need the procedure to evaluate the contribution of the controlled emission sources in the final environmental damage. The paper addresses some related problems.

The paper concerns a class of air pollution dispersion models, which can be applied as tools to support decisions in environment quality control by evaluating contribution of each source in the resulting pollution field and, ultimately, utilizing those data in

air quality control. It is assumed that pollution transport process can be considered as distributed parameters system, governed by the transport equation. Implementation discussed in the sequel is sulfur-oriented, but the approach can be applied in a more general class of the forecasting models.

The governing model generates short-term forecasts of air pollution related to a specified, complex emission field. Calculation of the transport of sulfur pollution is carried out by Lagrangian-type, three layer trajectory model [1, 2]. The mass balance for the pollutants is calculated for air parcels following the wind trajectories. The model takes into account two basic polluting components, SO_2 and SO_4^- . Transport equations include chemical transformations $SO_2 \implies SO_4^-$, dry deposition, scavenging by precipitation. The uniform space discretization step, $h = \Delta x = \Delta y$ is applied in the computational algorithm. Points along the trajectory are determined at discrete time moments, based on the interval τ . The main output constitutes the concentrations of SO_2 , averaged over the discretization element and the vertical layer height. The governing equations have the following form

$$\frac{\partial c}{\partial t} + \vec{u} \nabla c - K \Delta c + \gamma c = Q \quad \text{in} \quad \Omega \times (0, T), \quad (1)$$

along with the boundary conditions

$$c = c_0 \quad \text{on} \quad S^- = \{\partial\Omega \times (0, T) \mid \vec{u} \cdot \vec{n} < 0\} \quad \text{- inflow of the domain}, \quad (1a)$$

$$K \frac{\partial c}{\partial \vec{n}} = 0 \quad \text{on} \quad S^+ = \{\partial\Omega \times (0, T) \mid \vec{u} \cdot \vec{n} \geq 0\} \quad \text{- outflow of the domain}, \quad (1b)$$

and the initial condition

$$c(0) = c_0 \quad \text{in} \quad \Omega. \quad (1c)$$

where

Ω - domain considered, with the boundary $\partial\Omega = S^+ \cup S^-$,

$(0, T)$ - time interval of the forecast,

c - pollution concentration,

\vec{u} - wind velocity vector,

\vec{n} - normal vector of the domain Ω ,

K - horizontal/vertical diffusion coefficient,

γ - pollution reduction (due to deposition and chemical transformation) coefficient,

Q - total emission field.

The emission field on the right-hand side of (1) can be expressed in the following form:

$$Q(x, y, t) = q(x, y, t) + \sum_{i=1}^N \chi_i(x, y) q_i(t), \quad (2)$$

where

$q(x, y, t)$ - background (uncontrolled) emission field,

$q_i(t)$ - emission intensity of the controlled, i -th source,

$\chi_i(x, y)$ - characteristic function of the, i -th source.

The air quality damage is represented by an environmental cost function of the following form:

$$J(c) = \frac{1}{T} \int_0^T \int_{\Omega} w(x, y) [\max(c(x, y, t) - c_{ad}(x, y, t))]^2 d\Omega dt, \quad (3)$$

where $w(x, y)$ denotes the area weight function that represents sensitivity of the domain to the specific type of air pollution. The component c_{ad} is the admissible level of concentration, which should not be violated.

Environmental cost function (3), due to the transport equation (1), implicitly depends on the emission intensity of the controlled sources. To implement emission control procedure, one has to evaluate quantitatively, according to the measure (3), the impact of each of the sources. A direct method is based on the consecutive reduction of emission level of the sources under question, and calculation of the related decrease of environmental cost index (3). This method requires, however, that the main transport equation must be consecutively solved for all the sources considered. Thus, the most time-consuming step of the analysis has to be repeated many times.

Another approach, discussed in the sequel, utilizes the properties of the adjoint equation [3, 4], related to the state equation (1). Let $\vec{q}(t) = [q_1(t), \dots, q_N(t)]$ denotes the vector function representing emissions of the controlled sources. Environmental cost index (3) can be considered as a function of \vec{q} , which can be expressed as

$$J(q) = \frac{1}{T} \int_0^T \int_{\Omega} F(c(\vec{q})) d\Omega dt, \quad (4)$$

where subintegral function - F , according to (3), is expressed as

$$F(x, y, t) = w(x, y) [\max(c(x, y, t) - c_{ad}(x, y, t))]^2, \quad (5)$$

In order to evaluate sensitivity of the index (4) to the emission of the sources $q_i(t)$, ($i = 1, \dots, N$), the gradient of this function must be computed.

Denote by $\epsilon \vec{s}$ the linear part of a small change of the emission level, $\vec{q}_{\epsilon} = \vec{q} + \epsilon \vec{s}$, which by (1) implies the respective change of concentration level $c_{\epsilon} = c + \epsilon p$ (the respective linear part of this variation is ϵp). Consequently, the linear part of the variation of the cost function (4) can be expressed in the form

$$\delta J = \frac{\epsilon}{T} \int_0^T \int_{\Omega} \frac{\partial F}{\partial c} p d\Omega dt, \quad (6)$$

where, according to (5), the derivative of subintegral function is as follows:

$$\frac{\partial F}{\partial c}(x, y, t) = 2 w(x, y) [\max(c(x, y, t) - c_{ad}(x, y, t))], \quad (6a)$$

To calculate effectively (6), the value of function p - which is not given explicitly - must be known. Below the procedure is presented [3, 4] that allows to calculate this variation in one simulation run of the transport equation.

Substituting expressions

$$\vec{q}_\epsilon = \vec{q} + \epsilon$$

to (1), we get the boundary-initial problem, which should be satisfied by the increment p . The left-hand side of the equation obtained is identical as that of (1), while the right side depends on the emission increment, $\vec{s}(t) = [s_1(t), \dots, s_N(t)]$, and the initial-boundary conditions are homogeneous

$$\frac{\partial p}{\partial t} + \vec{u} \nabla p - K \Delta p + \gamma p = \sum_{i=1}^N \chi_i(x, y) s_i(t) \quad \text{in } \Omega \times (0, T), \quad (7)$$

$$p = 0 \quad \text{on } S^-, \quad (7a)$$

$$K \frac{\partial p}{\partial \vec{n}} = 0 \quad \text{on } S^+, \quad (7b)$$

$$p(0) = 0 \quad \text{in } \Omega. \quad (7c)$$

Both sides of equation (7) can be multiplied by respectively regular function $\varphi(x, y, t)$, where $\varphi \in L^2(0, T; H^1(\Omega))$, and then integrate the obtained equation in $\Omega \times (0, T)$. Utilizing next Gauss formula, we get the following integral identity:

$$\begin{aligned} & - \int_0^T \int_\Omega p \frac{\partial \varphi}{\partial t} d\Omega dt + \int_\Omega [p(T) \varphi(T) - p(0) \varphi(0)] d\Omega - \int_0^T \int_\Omega p (\vec{u} \cdot \nabla \varphi) d\Omega dt \\ & + \int_0^T \int_S p \varphi (\vec{u} \cdot \vec{n}) dS dt + K_H \int_0^T \int_\Omega \nabla p \cdot \nabla \varphi d\Omega dt - K_H \int_0^T \int_S \varphi \frac{\partial p}{\partial \vec{n}} dS dt \\ & + \gamma \int_0^T \int_\Omega p \varphi d\Omega dt = \int_0^T \int_\Omega \varphi \sum_{i=1}^N \chi_i s_i d\Omega dt \end{aligned} \quad (8)$$

Now we introduce the adjoint variable, p^* , defined as the solution of the following boundary-value problem:

$$-\frac{\partial p^*}{\partial t} - \vec{u} \nabla p^* - K \Delta p^* + \gamma p^* = \frac{\partial F}{\partial c}(c) \quad \text{in } \Omega \times (0, T), \quad (9)$$

along with the boundary conditions

$$p^* = 0 \quad \text{on } S^-, \quad (9a)$$

$$K \frac{\partial p^*}{\partial \vec{n}} + (\vec{u} \cdot \vec{n}) p^* = 0 \quad \text{on } S^+ \quad (9b)$$

and the final condition (for the end of the time interval)

$$p^*(T) = 0 \quad \text{in } \Omega. \quad (9c)$$

Equation (9), in comparison to (1), is solved for the reversed direction of wind, and the right-hand side is the derivative of the subintegral function of environmental index

(4). The meaning of the boundary conditions of the adjoint problem will be explained below.

Utilizing the same technique as for the state equation, we can multiply (9) by the respectively regular function $\psi \in L^2(0, T; H^1(\Omega))$ and integrate in $\Omega \times (0, T)$. Due to homogeneous boundary conditions in (9), some terms disappear and finally we get the following identity:

$$\begin{aligned} & - \int_0^T \int_{\Omega} \psi \frac{\partial p^*}{\partial t} d\Omega dt - \int_0^T \int_{\Omega} \psi (\vec{u} \cdot \nabla p^*) d\Omega dt + K_H \int_0^T \int_{\Omega} \nabla \psi \cdot \nabla p^* d\Omega dt \\ & - K_H \int_0^T \int_S \psi \frac{\partial p^*}{\partial \vec{n}} dS dt + \gamma \int_0^T \int_{\Omega} \psi p^* d\Omega dt = \int_0^T \int_{\Omega} \psi \frac{\partial F}{\partial c} d\Omega dt \end{aligned} \quad (10)$$

It can be shown [3] that the solutions to the boundary-value problems (7) and (9), p and p^* , respectively, are sufficiently regular functions that the substitutions $\varphi = p^*$ in (8) and $\psi = p$ in (10) are possible. Comparing the obtained integral equations we get the following identity:

$$\begin{aligned} \int_0^T \int_{\Omega} p \frac{\partial F}{\partial c} d\Omega dt &= \int_0^T \int_{\Omega} p^* \sum_{i=1}^N \chi_i s_i d\Omega dt - \int_{\Omega} [p(T)p^*(T) - p(0)p^*(0)] d\Omega \\ &- \int_0^T \int_S [p(p^*(\vec{u} \cdot \vec{n}) + K_H \frac{\partial p^*}{\partial \vec{n}}) - p^* K_H \frac{\partial p}{\partial \vec{n}}] dS dt \end{aligned} \quad (11)$$

Note, that due to the homogeneous boundary and initial conditions in (7) and (9), the last two terms in (11) are equal zero. Thus, substituting the obtained relation in (6) we can express the increment of the cost function in the following form

$$\begin{aligned} \delta J &= \frac{\epsilon}{T} \int_0^T \int_{\Omega} p^* \sum_{i=1}^N \chi_i s_i d\Omega dt = \frac{\epsilon}{T} \sum_{i=1}^N \int_0^T \int_{\Omega} p^* \chi_i d\Omega |s_i| dt \\ &= \frac{\epsilon}{T} \sum_{i=1}^N \int_0^T G_i(t) s_i(t) dt, \end{aligned} \quad (12)$$

where we denote

$$G_i(t) = \int_{\Omega} p^*(x, y, t) \chi_i(x, y) d\Omega, \quad i = 1, \dots, N. \quad (12a)$$

The last relation allows to calculate effectively the increment of the cost function, related to variation of the specific emission source. Our goal is to evaluate the contribution of each emission source in air quality deterioration. This contribution is calculated in the sense of the measure (4), as the respective component of the gradient of the cost function

$$\begin{aligned} \frac{\partial J}{\partial q_i} &= \lim_{\epsilon \rightarrow 0} \frac{\delta J}{\epsilon} = \frac{1}{T} \int_0^T G_i(t) s_i(t) dt \\ &= \frac{1}{T} \int_0^T \int_{\Omega} \chi_i(x, y) p^*(x, y, t) s_i(t) d\Omega dt, \quad (i = 1, \dots, N). \end{aligned} \quad (13)$$

Thus, to calculate the contribution of the emission sources one must in the sequel solve the problems (1), (7) and substitute the adjoint variable p^* to (8). This contribution is calculated in the sense of the measure (4), as the respective component of the gradient of the cost function. To get the final solution, the transport and the adjoint equations must be solved only once.

The method presented above has been applied for the real-data case study concerning the Upper Silesia region. Evaluation of the environmental impact of the major power plants has been performed by the adjoint variable algorithm.

2 Test computations

The test calculations were performed for the set of 27 major power plants in the Upper Silesia and Krakow region in Poland. Locations of the sources are indicated in Figures 1-5. The rectangle domain $110 \text{ km} \times 74 \text{ km}$ is discretized by the uniform grid with the space step $h = 2 \text{ km}$. Grid coordinates and the main parameters of the controlled emission sources are shown in Table 1.

The aim of the computational experiment was to evaluate and compare the environmental impact of each source by the adjoint variable method, discussed in the previous section. The area weight function was set to 1 for the Kraków city domain and 0 – outside. Thus, we were to calculate environmental impact of the sources under consideration to this domain (indicated in Figures 1 – 5). To evaluate accuracy of the results obtained by the adjoint variable algorithm, the reference contributions of the emission sources were calculated. The relative contribution of a specific source is obtained as the solution to (1) for the emission of this source reduced by 50% in the total emission field.

The computed (by the adjoint variable method) and the reference results for 27 sources discussed are presented in Tables 2 – 5. They represent, respectively, four 3-month periods of the year under consideration (1996). Figures 2,5 refer to the Winter quarters and Figures 3,4 – to the Summer quarters, respectively. Two columns of each table present the computed result (obtained by the adjoint variable method) and the reference data (obtained by the direct calculation). Both groups of results show the dominating impact of the source No. 22 (Skawina power plant) and the intermediate contribution of sources No. 10, 20, 21. The correlation coefficient of two sets of results is about $R=0.97$ for all cases.

Figures 1 – 4 present the respective resulting maps of a long-term forecasts of SO_2 concentration and the related maps of the adjoint variable distribution, calculated according to (7), for the reversed direction of time. The relative impact of the analyzed emission sources was computed, using relations (8) – (9), as the gradient components of the environmental cost function (4).

Figure 5 presents the respective pair of maps obtained for the short-term (3 days) forecast. It illustrates more directly relation between SO_2 concentration map and distribution of the respective adjoint variable.

Table 1. List of the controlled emission sources

Source number	Source coordinates	Stack height [m]	Emission – winter [kg/h]	Emission – summer [kg/h]
1	(14,2)	160	426.91	256.15
2	(18,31)	95	94.89	63.25
3	(18,31)	135	132.82	31.63
4	(15,1)	250	426.91	189.74
5	(12,27)	100	363.66	180.25
6	(8,25)	110	569.24	379.48
7	(20,23)	152	284.61	158.12
8	(21,24)	100	573.60	379.48
9	(21,24)	120	664.08	426.91
10	(21,24)	300	6324.60	4743.45
11	(13,25)	250	1106.81	790.58
12	(18,31)	160	948.69	695.71
13	(18,31)	200	1359.79	1011.94
14	(8,20)	200	1660.21	1185.86
15	(8,20)	160	758.95	505.97
16	(8,20)	100	727.33	505.97
17	(46,12)	260	1106.81	790.58
18	(14,17)	68	161.28	117.01
19	(1,20)	300	4711.83	3510.15
20	(30,23)	150	1929.00	1423.04
21	(30,23)	260	2055.49	1739.27
22	(43,11)	120	1992.25	1296.55
23	(9,31)	110	164.44	113.84
24	(9,31)	120	170.76	110.68
25	(13,19)	120	240.33	177.09
26	(2,29)	60	205.55	158.12
27	(2,29)	120	221.36	145.47

Table 2. Computed and the reference contribution of emission sources (January – March 1996)

No	Com- puted	Refe- rence	No	Com- puted	Refe- rence	No	Com- puted	Refe- rence
1	1.22	0.13	10	31.65	9.59	19	3.87	0.50
2	0.08	0.16	11	2.39	0.78	20	34.41	6.41
3	0.11	0.20	12	0.63	0.89	21	40.44	4.14
4	2.07	0.01	13	3.17	1.33	22	204.49	59.95
5	0.30	0.22	14	1.79	0.17	23	0.08	0.05
6	0.54	0.26	15	0.81	0.11	24	0.09	0.04
7	0.54	0.48	16	0.77	0.24	25	0.29	0.05
8	0.81	1.00	17	7.67	0.08	26	0.15	0.04
9	1.16	0.44	18	0.20	0.05	27	0.16	0.04

Table 3. Computed and the reference contribution of emission sources (April – June 1996)

No	Com- puted	Refe- rence	No	Com- puted	Refe- rence	No	Com- puted	Refe- rence
1	0.20	0.35	10	10.71	6.44	19	6.04	3.50
2	0.05	0.26	11	1.14	1.50	20	12.70	16.23
3	0.03	0.14	12	0.55	1.94	21	18.80	15.08
4	0.43	0.10	13	0.77	2.42	22	77.31	67.59
5	0.24	0.63	14	1.21	2.06	23	0.12	0.24
6	0.48	1.06	15	1.09	0.87	24	0.10	0.23
7	0.43	0.49	16	0.71	1.27	25	0.33	0.44
8	1.04	0.31	17	9.46	1.08	26	0.12	0.25
9	1.36	0.48	18	0.23	0.28	27	0.12	0.24

Table 4. Computed and the reference contribution of emission sources (July – September 1996)

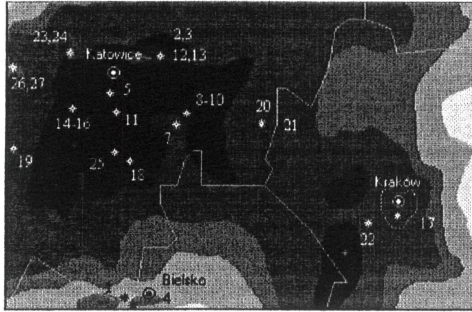
No	Com- puted	Refe- rence	No	Com- puted	Refe- rence	No	Com- puted	Refe- rence
1	0.43	0.50	10	33.82	13.20	19	1.39	1.05
2	0.07	0.12	11	4.01	1.26	20	20.28	13.72
3	0.04	0.08	12	1.32	1.13	21	21.00	11.43
4	0.40	0.05	13	2.64	0.81	22	156.53	72.17
5	0.22	0.44	14	0.89	0.25	23	0.12	0.12
6	0.37	0.33	15	0.47	0.14	24	0.09	0.09
7	0.22	0.77	16	0.43	0.40	25	0.18	0.18
8	0.61	0.80	17	12.08	0.62	26	0.11	0.11
9	1.13	1.01	18	0.11	0.05	27	0.08	0.08

Table 5. Computed and the reference contribution of emission sources (October – December 1996)

No	Com- puted	Refe- rence	No	Com- puted	Refe- rence	No	Com- puted	Refe- rence
1	0.53	0.11	10	23.26	4.44	19	2.21	1.03
2	0.19	0.23	11	1.57	0.50	20	22.08	5.96
3	0.28	0.21	12	1.79	1.17	21	25.09	4.43
4	1.62	0.02	13	2.33	1.59	22	230.75	62.49
5	0.21	0.28	14	1.15	0.31	23	0.10	0.06
6	0.26	0.32	15	0.47	0.16	24	0.11	0.06
7	0.75	0.24	16	0.46	0.31	25	0.18	0.08
8	0.83	1.10	17	0.05	0.02	26	0.06	0.06
9	1.07	0.88	18	0.14	0.06	27	0.06	0.07

SO₂ concentration forecast

Layer 1

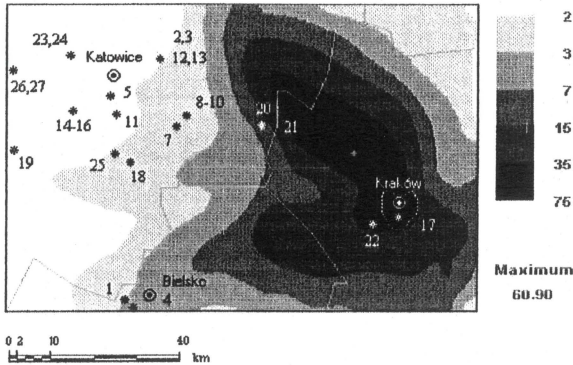


Initial date 01/01/96

Time horizon 92 days

Distribution of the adjoint variable

Layer 3



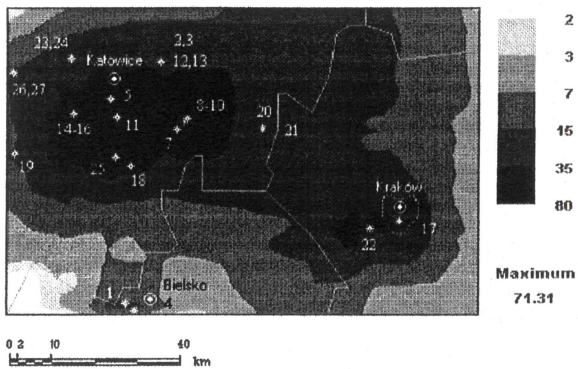
Initial date 01/01/96

Time horizon 92 days

Figure 1: The averaged (January-March) SO_2 concentration forecast [$\mu g/m^3$] (top), and the adjoint variable distribution (bottom)

SO2 concentration forecast

Layer 1

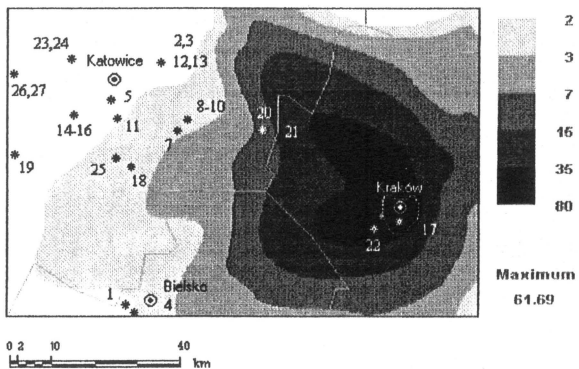


Initial date 01/04/96

Time horizon 92 days

Distribution of the adjoint variable

Layer 3



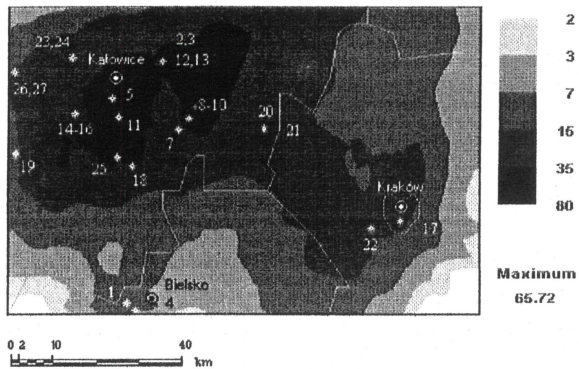
Initial date 01/04/96

Time horizon 92 days

Figure 2: The averaged (April-June) SO_2 concentration forecast [$\mu\text{g}/\text{m}^3$] (top), and the adjoint variable distribution (bottom)

SO2 concentration forecast

Layer 1

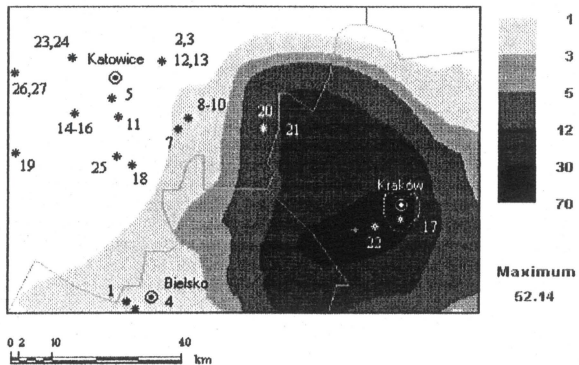


Initial date 01/07/96

Time horizon 92 days

Distribution of the adjoint variable

Layer 3

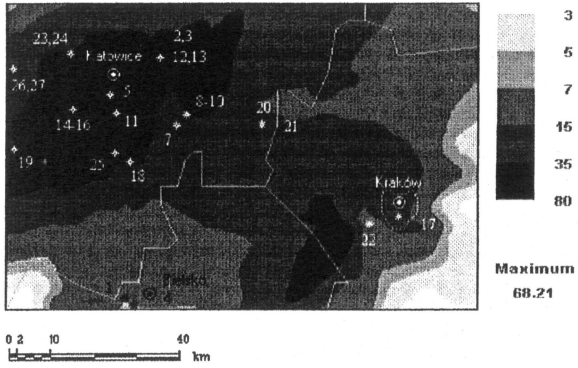


Initial date 01/07/96

Time horizon 92 days

Figure 3: The averaged (July-September) SO_2 concentration forecast [$\mu g/m^3$] (top), and the adjoint variable distribution (bottom)

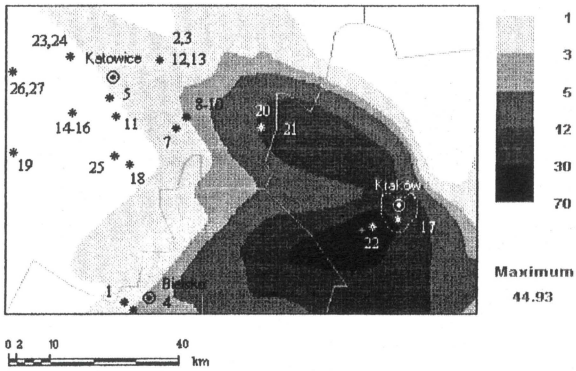
Season-averaged concentration forecast Layer 1



Initial date 01/10/96

Time horizon 92 days

Distribution of the adjoint variable Layer 3



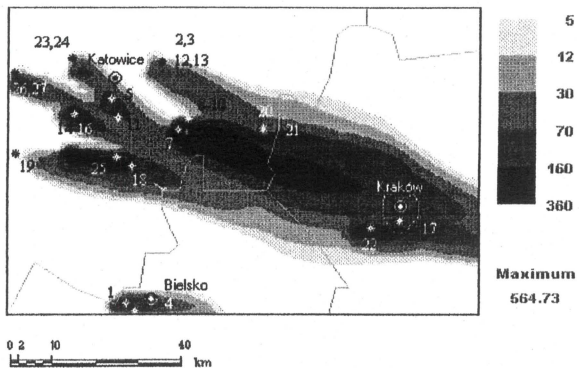
Initial date 01/10/96

Time horizon 92 days

Figure 4: The averaged (October-December) SO_2 concentration forecast [$\mu\text{g}/\text{m}^3$] (top), and the adjoint variable distribution (bottom)

Short-term concentration forecast

Layer 1

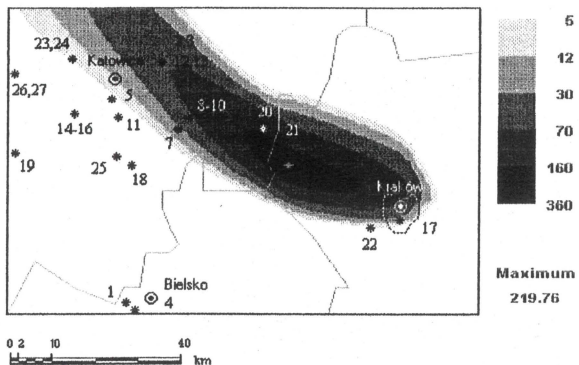


Initial date 01/10/96

Time horizon 3 days

Distribution of the adjoint variable

Layer 3



Initial date 01/10/96

Time horizon 3 days

Figure 5: Short-term (3 days) SO_2 concentration forecast [$\mu g/m^3$] (top), and the adjoint variable distribution (bottom)

References

- [1] Holnicki P., Kałuszko A., Żochowski A.: A microcomputer implementation of air quality forecasting system for urban scale. *Microcomputer Applications*, vol. 13, No. 2 1994, pp. 76–84.
- [2] Holnicki P., Żochowski A., and Aleksander Warchałowski A. (2001) Regional-scale air pollution dispersion model. *Environment Protection Engineering* 33, 133-145.
- [3] Lyons J.L.: *Optimal Control of Systems Governed by Partial Differential Equations*. Springer Verlag, Berlin 1971.
- [4] Marchuk G.I.: *Adjoint Equations and Analysis of Complex Systems*. Kluwer Academic Publishers, Dordrecht 1995.
- [5] Uliasz M.: Lagrangian particle dispersion modeling in mesoscale applications. *Environment Modeling* – vol 2 (ed. P. Zannetti). Computational Mechanics Publications, Southampton 1994, pp. 71 – 100.

